Synthesis, Characterisation and Crystal Structures of a Series of Pentanuclear Arene-substituted Clusters *

Jack Lewis,[a] **Chi-Keung Li,**[a] **M. Carmen Ramirez de Arellano,**[a] **Paul R. Raithby**[a] **and Wing-Tak Wong**[b]

[a] *University Chemical Laboratory, Lensfield Road, Cambridge CB2 1EW, UK*

[b] *Department of Chemistry, The University of Hong Kong, Pokfulam Road, Hong Kong*

Reduction of the tetraosmium cluster $[Os_4H_4(CO)_{12}]$ with K–Ph_2CO gave the cluster dianion $[Os_4H_4(CO)_{11}]^{2-}$ **1** in quantitative yield. This dianion was treated with $[Ru(C_6H_6)(MeCN)_3]^{2+}$ to give $[RuOs_4H_4(\eta^6\text{-}C_6H_6)(CO)_{11}]$ **2** in fair yield, while the corresponding reaction with $[Os(C_6H_6)(MeCN)_3]^{2+}$ gave $[Os_5H_4(\eta^6\text{-}C_6H_6)(CO)_{11}]$ **3** and $[Os_5H_4(\eta^6\text{-}C_6H_6)(CO)_{12}]$ **4** in similar yields (*ca.* 25% each). Clusters **2**–**4** have been fully characterised by both spectroscopic and crystallographic methods. The crystal structures of **2** and **3** are *isomorphous* and both the molecules are isostructural. Both contain a trigonal-bipyramidal metal-core geometry with the η^6-C_6H_6 co-ordinated to the Ru or Os atom in an equatorial position. Cluster **4** contains an Os_4 tetrahedron with one Os–Os edge bridged by an '$Os(\eta^6\text{-}C_6H_6)(CO)$' unit. Complex **3** is not convertible into **4** under thermolytic and photolytic conditions in the presence of CO, or **4** into **3** in the absence of CO.

The chemistry of arenemetal carbonyl clusters has been extensively studied. We have been able to synthesise a wide range of arene-containing ruthenium and osmium carbonyl clusters with a variety of structural units. In these clusters (Ru_3,[1] Os_3,[2] $RuOs_3$,[3] Os_4,[4] Ru_5C[5] and Ru_6C[6]) two modes of co-ordination of benzene to the metal cluster have been observed.[1–6] A conventional η^6 bonding mode as in $[Os_4H_2(CO)_{10}(C_6H_6)]$[4] and $[Ru_6C(CO)_{14}(arene)]$[7] is most commonly observed. However, the μ_3-$\eta^2:\eta^2:\eta^2$ (face capping) mode which occurs in $[M_3(CO)_9(C_6H_6)]$ (M = Ru[1] or Os[2]), $[Ru_5C(CO)_{12}(C_6H_6)]$[5] and $[Ru_6C(CO)_{11}(C_6H_6)_2]$[6a] is interesting due to the potential relevance to the chemisorption of benzene on metal surfaces. We have reported some interesting dynamic behaviour of some of these co-ordinated benzene molecules in both solution and solid state.[6,8] Under carefully chosen conditions, we have observed a change in bonding mode from face-capping $\eta^2:\eta^2:\eta^2$ to η^6-terminal.[2b,5]

As part of our continuing efforts in the studies of arene interaction with metal clusters, we report here a new synthetic route to a new class of pentanuclear benzene cluster based on the reaction between $[M(C_6H_6)(MeCN)_3]^{2+}$ (M = Ru or Os) and the dianion $[Os_4H_4(CO)_{11}]^{2-}$ which can be derived from $[Os_4H_4(CO)_{12}]$.

Results and Discussion

The tetranuclear cluster $[Os_4H_4(CO)_{12}]$ was treated with an excess of potassium–benzophenone in tetrahydrofuran (thf) at ambient temperature to give an air-sensitive yellow dianionic cluster $[Os_4H_4(CO)_{11}]^{2-}$ **1**, which was not isolated but characterised by both IR and ^1H NMR spectroscopies (see Table 1). Treatment of **1** with an *excess* of $[Ru(C_6H_6)(MeCN)_3][BF_4]_2$ in dichloromethane at room temperature for 30 min gives a red compound $[RuOs_4(\eta^6\text{-}C_6H_6)(CO)_{11}]$ **2** in *ca.* 20% yield after chromatographic separation on silica. At least three other benzene-containing clusters are formed in the same reaction but in very low yields; the full characterisation of these products is precluded by their low availability. The benzene cluster **2** was first characterised by IR, ^1H NMR and mass spectroscopy. A singlet at δ 5.98 in the ^1H NMR spectrum indicates the presence of a η^6-terminally bonded benzene fragment in **2**. This chemical shift is comparable to the value observed for $[RuOs_3(CO)_9(MeC_2Me)(\eta^6\text{-}C_6H_6)]$ (δ 5.58).[3] The spectrum shows no change in the chemical shift of benzene in the temperature range 215–320 K and there appears to be no evidence for benzene migration over the cluster surface on the NMR time-scale. Three hydride signals are observed at δ −15.19, −15.60 and −19.03 with relative intensity 1:2:1, which is consistent with the solid-state structure of **2**. The corresponding reaction of anion **1** with $[Os(C_6H_6)(MeCN)_3][BF_4]_2$ gives two major products in approximately the same yields (*ca.* 25% each). A red compound $[Os_5H_4(\eta^6\text{-}C_6H_6)(CO)_{11}]$ **3** analogous to **2** was characterized by IR, ^1H NMR and mass spectroscopy. The ^1H NMR spectrum is very similar to that of **2**. A strong singlet at δ 6.08, implying a terminally η^6-co-ordinated benzene as in the case of **2**, was found. A green compound was characterised by IR, ^1H NMR spectroscopy and X-ray analysis as $[Os_5H_4(\eta^6\text{-}C_6H_6)(CO)_{12}]$ **4**. However both electron-impact and fast atom bombardment techniques fail to produce a good mass spectrum for this molecule. The ^1H NMR spectrum reveals the presence of a terminally bonded benzene (δ 6.05) and four hydrides (δ −12.03, −12.85, −18.19, −20.00) in different environments. Single crystals of **2**–**4** suitable for X-ray work were obtained by slow evaporation of CH_2Cl_2–hexane solutions at ambient temperature over several days.

The crystal structures of compounds **2** and **3** are isomorphous, and the molecular structures are very closely related. The structures are shown in Figs. 1 and 2, respectively, together with the labelling schemes. Relevant bond distances and angles are listed in Tables 2 (for **2**) and 3 (for **3**). Both molecules consist of a trigonal bipyramidal metal core. The metal–metal distances range from 2.744(2) to 2.888(2) Å for both species, and are similar to those observed in other arene clusters such as $[Os_4H_2(\eta^6\text{-}C_6H_6)(CO)_{10}]$[4] and $[RuOs_3(CO)_9(MeC_2Me)(\eta^6\text{-}C_6H_6)]$.[3] The η^6-benzene ligand is co-ordinated to the unique Ru atom which lies in the trigonal plane of the cluster core in **2**. An essentially identical co-ordination is observed in **3**. The hydride atoms cannot be located directly by direct X-ray analysis. However, potential-energy calculations[9] suggest they bridge the Ru–Os(3), Os(1)–Os(3), Os(2)–Os(3) and Os(3)–

---

* *Supplementary data available:* see Instructions for Authors, *J. Chem. Soc., Dalton Trans.*, 1993, Issue 1, pp. xxiii–xxviii.

Table 1 Spectroscopic data for the dianion $[Os_4H_4(CO)_{11}]^{2-}$ **1** and the clusters $[RuOs_4H_4(\eta^6\text{-}C_6H_6)(CO)_{11}]$ **2**, $[Os_5H_4(\eta^6\text{-}C_6H_6)(CO)_{11}]$ **3** and $[Os_5H_4(\eta^6\text{-}C_6H_6)(CO)_{12}]$ **4**

Compound	IR (cm^{-1}), ν(CO)	^{1}H NMR (δ)	Mass spectrum, *m/z*
1	[a] 2047w, 1968s, 1923w	[b] −20.41 (s, 1 H), −20.75 (s, 1 H) −21.32 (s, 1 H), −22.26 (s, 1 H)	
2	[c] 2078w, 2068w, 2050vs, 2031s, 2017s, 1987m	[d] 5.98 (s, 6 H), −15.19 (s, 1 H) −15.60 (s, 2 H), −19.03 (s, 1 H)	1252 (1252)[e]
3	[c] 2076w, 2067w, 2050vs, 2029s, 2019s, 1986m	[d] 6.08 (s, 6 H), −14.50 (s, 1 H) −15.94 (s, 2 H), −20.21 (s, 1 H)	1341 (1341)[e]
4	[e] 2084m, 2048s, 2028m, 2015vs, 1985w	[d] −6.05 (s, 6 H), −12.03 (s, 1 H), −12.85 (s, 1 H), −18.19 (s, 1 H) −20.00 (s, 1 H)	

[a] Recorded in thf. [b] Recorded in [$^2H_8$]tetrahydrofuran. [c] Recorded in CH_2Cl_2. [d] Recorded in $CDCl_3$ at 297 K. [e] Calculated value.

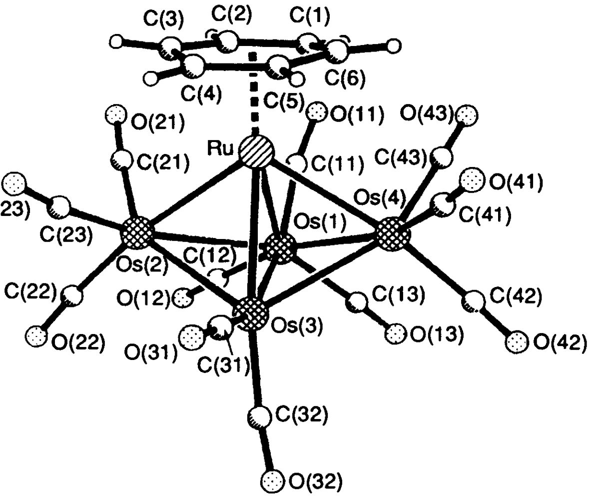

Fig. 1 The molecular structure of $[RuOs_4H_4(\eta^6\text{-}C_6H_6)(CO)_{11}]$ **2**

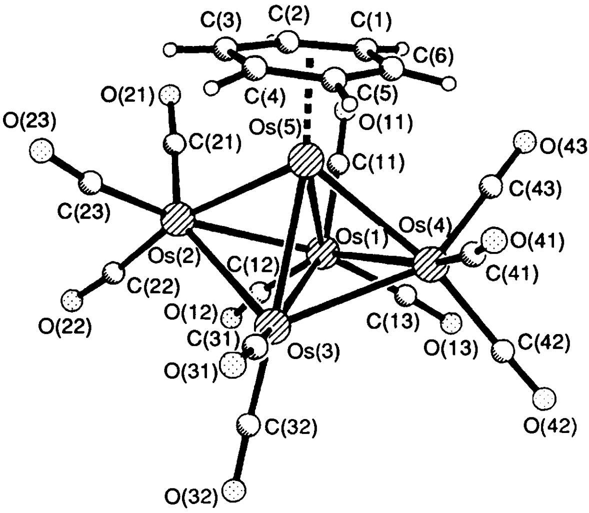

Fig. 2 The molecular structure of $[Os_5H_4(\eta^6\text{-}C_6H_6)(CO)_{11}]$ **3**

Table 2 Selected bond lengths (Å) and angles (°) for compound **2**

Os(1)–Ru	2.803(3)	Os(3)–Os(4)	2.863(3)
Os(2)–Ru	2.744(3)	Ru–C(1)	2.22(5)
Os(3)–Ru	2.885(3)	Ru–C(2)	2.27(4)
Os(4)–Ru	2.756(3)	Ru–C(3)	2.33(4)
Os(1)–Os(2)	2.804(2)	Ru–C(4)	2.26(4)
Os(1)–Os(3)	2.887(2)	Ru–C(5)	2.22(4)
Os(1)–Os(4)	2.806(2)	Ru–C(6)	2.29(4)
Os(2)–Os(3)	2.857(2)		
Os(1)–Ru–Os(3)	60.7(1)	Os(2)–Ru–Os(3)	60.9(1)
Os(1)–Ru–Os(3)	61.0(1)	Os(2)–Ru–Os(4)	111.1(1)
Os(1)–Ru–Os(4)	60.6(1)	Os(3)–Ru–Os(4)	60.9(1)

Table 3 Selected bond lengths (Å) and angles (°) for compound **3**

Os(1)–Os(2)	2.814(2)	Os(1)–Os(3)	2.888(2)
Os(1)–Os(4)	2.808(2)	Os(1)–Os(5)	2.796(2)
Os(2)–Os(3)	2.872(2)	Os(2)–Os(5)	2.753(2)
Os(3)–Os(4)	2.868(3)	Os(3)–Os(5)	2.874(2)
Os(4)–Os(5)	2.743(2)	Os(5)–C(1)	2.23(6)
Os(5)–C(2)	2.27(6)	Os(5)–C(3)	2.34(5)
Os(5)–C(4)	2.26(4)	Os(5)–C(5)	2.29(5)
Os(5)–C(6)	2.26(5)		
Os(1)–Os(5)–Os(2)	60.9(1)	Os(1)–Os(5)–Os(3)	61.2(1)
Os(2)–Os(5)–Os(3)	61.4(1)	Os(1)–Os(5)–Os(4)	60.9(1)
Os(2)–Os(5)–Os(4)	111.8(1)	Os(3)–Os(5)–Os(4)	61.4(1)

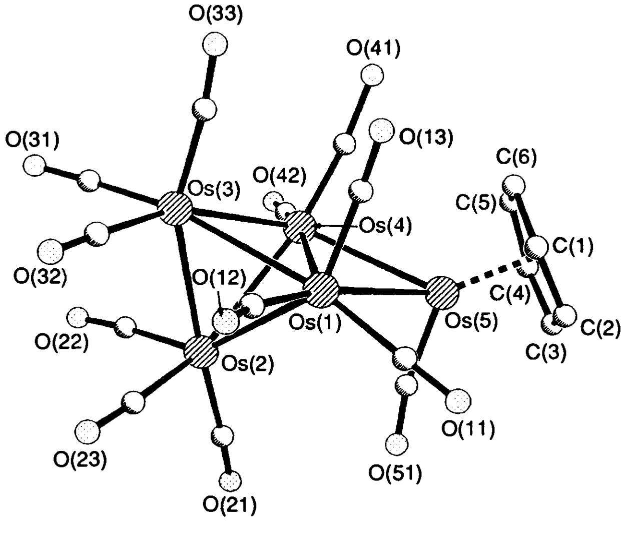

Fig. 3 The molecular structure of $[Os_5H_4(\eta^6\text{-}C_6H_6)(CO)_{12}]$ **4**

Os(4) edges in **2** and Os(3)–Os(5), Os(1)–Os(3), Os(2)–Os(3) and Os(3)–Os(4) edges in **3** respectively. Therefore, the molecules **2** and **3** both exhibit an approximately C_s symmetry. The molecular structure of **4** is shown in Fig. 3, and consists of a tetrahedral metal core with one '$Os(\eta^6\text{-}C_6H_6)(CO)$' unit bridged across one edge. The Os–Os distances [2.793(2)–2.974(2) Å] (Table 4) are within the range commonly observed in other pentaosmium carbonyl clusters. The positions of the four hydride atoms, as evident from the ^{1}H NMR spectrum, cannot be determined directly from the X-ray analysis. However, potential-energy calculations[9] suggest that the edges Os(1)–Os(2), Os(2)–Os(4), Os(3)–Os(4) and Os(4)–Os(5) are each bridged by a hydride. All the spectroscopic data for **4** are fully consistent with the observed solid-state structure established by X-ray analysis.

Although the dications $[M(C_6H_6)(MeCN)_3]^{2+}$ (M = Ru or Os) are frequently employed in the synthesis of benzene-containing clusters *via* the reaction with dianionic clusters, little is known about the mechanistic aspects of these reactions. From this work it is likely that the dianion $[Os_4H_4(CO)_{11}]^{2-}$ interacts with $[M(C_6H_6)(MeCN)_3]^{2+}$ to give an intermediate species $[MOs_4H_4(CO)_{11}(\eta^6\text{-}C_6H_6)(MeCN)]$ **5** which contains a μ-bridging metal–benzene fragment. The subsequent metal-core rearrangement of **5** coupled with loss of the co-ordinated MeCN gives the observed products **2** (for M = Ru) and **3** (for M = Os). The trapping of intermediate **5** by scavenging of CO in the reaction mixture yields the green product **4** in the case of osmium. The change from a trigonal-bipyramidal to an edge-bridged tetrahedral arrangement has been reported for the nucleophilic addition of CO, $P(OMe)_3$, or I^- to $[Os_5H_2(CO)_{15}]$.[10] However, **3** and **4** are not interconvertible under thermal or photochemical conditions. Heating of a CH_2Cl_2 solution of **4** for 12 h gives no observable change. Photolysis of **4** in CH_2Cl_2 gives only intractable decomposition products. Furthermore, we have no evidence that **3** reacts with CO in solution to give **4**. The probable mechanism for the formation of **2**–**4** is depicted in Scheme 1.

Table 4 Selected bond lengths (Å) and angles (°) for compound **4**

Os(1)–Os(2)	2.974(2)	Os(4)–Os(5)	2.849(2)
Os(1)–Os(3)	2.919(2)	Os(5)–C(1)	2.21(4)
Os(1)–Os(4)	2.813(2)	Os(5)–C(2)	2.27(5)
Os(1)–Os(5)	2.929(2)	Os(5)–C(3)	2.17(5)
Os(2)–Os(3)	2.793(2)	Os(5)–C(4)	2.21(6)
Os(2)–Os(4)	2.963(2)	Os(5)–C(5)	2.29(5)
Os(3)–Os(4)	2.804(2)	Os(5)–C(6)	2.34(5)
Os(2)–Os(1)–Os(3)	56.6(1)	Os(2)–Os(3)–Os(4)	63.9(1)
Os(2)–Os(1)–Os(4)	61.5(1)	Os(1)–Os(4)–Os(2)	61.9(1)
Os(2)–Os(1)–Os(5)	95.9(1)	Os(1)–Os(4)–Os(3)	62.6(1)
Os(3)–Os(1)–Os(4)	58.6(1)	Os(1)–Os(4)–Os(5)	62.3(1)
Os(3)–Os(1)–Os(5)	117.9(1)	Os(2)–Os(4)–Os(3)	57.9(1)
Os(4)–Os(1)–Os(5)	59.5(1)	Os(2)–Os(4)–Os(5)	97.9(1)
Os(1)–Os(2)–Os(3)	60.7(1)	Os(3)–Os(4)–Os(5)	124.8(1)
Os(1)–Os(2)–Os(4)	56.6(1)	Os(1)–Os(5)–Os(4)	58.2(1)
Os(3)–Os(2)–Os(4)	58.2(1)	Os(5)–C(51)–O(51)	168.5(1)
Os(1)–Os(3)–Os(2)	62.7(1)		

Table 6 Atomic coordinates (× 10^4) for $[RuOs_4H_4(\eta^6\text{-}C_6H_6)(CO)_{11}]$ **2**

Atom	x	y	z
Os(1)	874(1)	1049(1)	1561(1)
Os(2)	1307(2)	239(1)	3340(1)
Os(3)	3338(1)	94(1)	1957(1)
Os(4)	3570(2)	1533(1)	1147(1)
Ru	3068(3)	1409(2)	3103(2)
C(11)	131(45)	1959(28)	1921(27)
C(12)	−850(42)	560(24)	1604(24)
C(13)	551(36)	1130(21)	129(22)
C(21)	82(46)	858(27)	3891(28)
C(22)	65(41)	−574(24)	3281(23)
C(23)	2300(41)	−107(23)	4527(26)
C(31)	5097(39)	−326(22)	2593(22)
C(32)	3156(30)	−636(19)	1007(19)
C(41)	5551(48)	1766(26)	1412(26)
C(42)	3609(45)	1500(26)	−260(28)
C(43)	2976(40)	2543(24)	1061(23)
O(11)	−203(35)	2600(17)	2063(25)
O(12)	−1988(30)	261(15)	1581(23)
O(13)	283(30)	1144(17)	−687(17)
O(21)	−702(39)	1288(20)	4215(25)
O(22)	−660(28)	−1084(22)	3184(21)
O(23)	2998(34)	−237(16)	5248(18)
O(31)	5999(26)	−615(19)	3006(20)
O(32)	3118(29)	−1041(16)	364(15)
O(41)	6655(32)	1939(23)	1622(23)
O(42)	3557(44)	1454(21)	−1090(18)
O(43)	2531(31)	3131(19)	999(18)
C(1)	2875(44)	2603(26)	3386(27)
C(2)	2137(45)	2231(25)	4107(25)
C(3)	2883(44)	1716(26)	4755(27)
C(4)	4345(45)	1509(26)	4637(27)
C(5)	5047(43)	1894(25)	3940(25)
C(6)	4365(37)	2476(22)	3342(22)

Table 5 Crystal data and data-collection parameters * for structures **2**–**4**

Compound	**2**	**3**	**4**
Formula	$C_{17}H_{10}O_{11}Os_4Ru$	$C_{17}H_{10}O_{11}Os_5$	$C_{18}H_{10}O_{12}Os_5$
M	1252.1	1341.3	1369.3
Crystal colour, habit	Black block	Black block	Black block
Crystal size (mm)	0.24 × 0.34 × 0.46	0.24 × 0.36 × 0.38	0.32 × 0.34 × 0.36
Crystal system	Monoclinic	Monoclinic	Orthorhombic
Space group	$P2_1/n$	$P2_1/n$	$P2_12_12_1$
a/Å	9.384(3)	9.381(2)	11.214(4)
b/Å	18.237(5)	18.198(4)	14.271(4)
c/Å	13.512(3)	13.505(3)	15.216(4)
β/°	97.78(2)	97.85(2)	—
U/Å^3	2291(1)	2284(1)	2435(2)
Z	4	4	4
D_c/g cm^{-3}	3.630	3.900	3.735
F(000)	2192	2320	2436
μ(Mo-Kα)/cm^{-1}	228.01	277.68	260.96
2θ Range/°	5.0–45.0	5.0–45.0	2.0–46.0
Scan speed/° min^{-1}	3.0–19.53	3.0–19.53	1.37–8.24
Scan range (ω)/°	1.60 plus Kα separation	1.60 plus Kα separation	0.70 + 0.34tanθ
Reflections measured	3391	3457	1955
Unique reflections	3017	3010	1955
Observed reflections	2139 [$F > 4\sigma(F)$]	2027 [$F > 4\sigma(F)$]	1663 [$F > 3\sigma(F)$]
Weighting scheme	$[\sigma^2(F) + 0.002(F)^2]^{-1}$	$[\sigma^2(F) + 0.002(F)^2]^{-1}$	$4F^2/[\sigma^2(F)^2 + (0.04F^2)^2]$
R	0.067	0.064	0.057
R'	0.079	0.075	0.067

* Details in common: T = 298 K; Mo-Kα radiation (λ = 0.710 69 Å); ω–2θ scan mode; background measurement, stationary crystal–stationary counter at beginning and end of scan, each for 25% of total scan time.

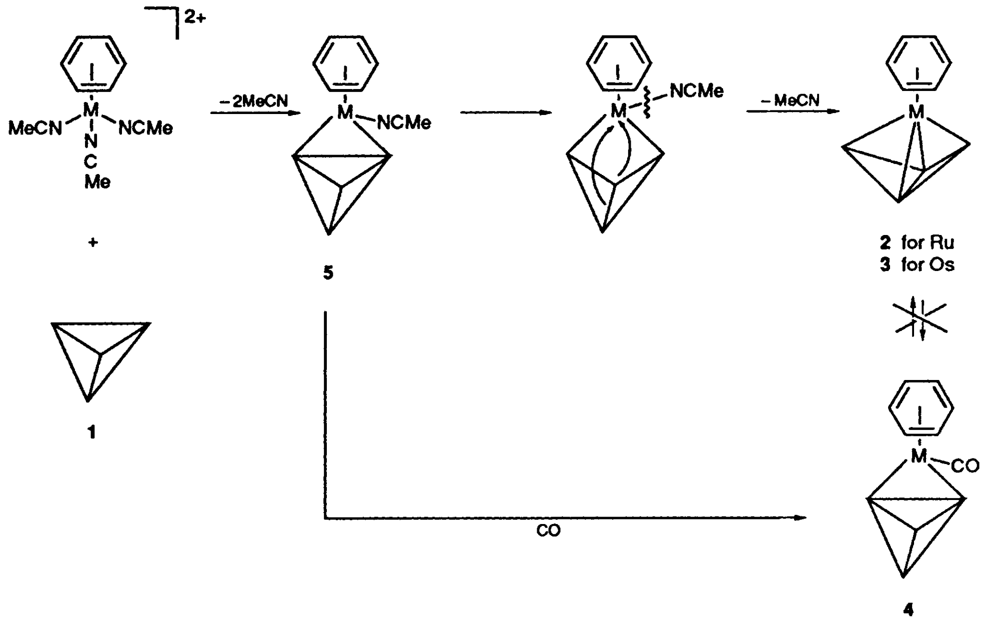

Scheme 1 Possible mechanistic pathway for the formation of compounds 2–4

Table 7 Atomic coordinates (× 10^4) for [$Os_5H_4(\eta^6\text{-}C_6H_6)(CO)_{11}$] 3

Atom	*x*	*y*	*z*
Os(1)	887(2)	8 944(1)	1 571(1)
Os(2)	3 589(2)	8 458(1)	1 155(1)
Os(3)	3 350(2)	9 904(1)	1 968(1)
Os(4)	1 312(2)	9 754(1)	3 357(1)
Os(5)	3 087(2)	8 589(1)	3 108(1)
C(1)	2 228(58)	7 716(30)	4 023(38)
C(2)	2 962(55)	7 361(32)	3 396(41)
C(3)	4 481(49)	7 517(29)	3 301(35)
C(4)	5 065(47)	8 098(26)	4 007(32)
C(5)	4 418(56)	8 452(33)	4 651(40)
C(6)	2 987(55)	8 285(30)	4 718(38)
C(11)	116(51)	8 015(30)	1 837(36)
O(11)	−247(35)	7 424(19)	2 035(28)
C(12)	603(47)	8 877(27)	142(36)
O(12)	278(31)	8 858(17)	−698(22)
C(13)	−863(42)	9 429(23)	1 621(27)
O(13)	−1 965(32)	9 745(17)	1 575(22)
C(21)	2 969(38)	7 542(23)	1 061(26)
O(21)	2 555(34)	6 911(19)	973(27)
C(22)	3 492(64)	8 514(36)	−236(48)
O(22)	3 554(45)	8 515(26)	−1 132(25)
C(23)	5 593(49)	8 212(27)	1 343(33)
O(23)	6 753(32)	7 995(25)	1 554(31)
C(31)	4 910(40)	10 340(23)	2 641(27)
O(31)	6 004(43)	10 627(23)	3 008(24)
C(32)	3 190(43)	10 621(25)	1 018(30)
O(32)	3 088(32)	11 086(17)	393(21)
C(41)	2 394(42)	10 101(23)	4 531(29)
O(41)	3 092(38)	10 260(21)	5 247(27)
C(42)	26(50)	10 627(30)	3 231(33)
O(42)	−646(42)	11 129(24)	3 214(31)
C(43)	68(56)	9 135(31)	3 911(38)
O(43)	−756(42)	8 725(22)	4 227(31)

Table 8 Atomic coordinates for [$Os_5H_4(\eta^6\text{-}C_6H_6)(CO)_{12}$] 4

Atom	*x*	*y*	*z*
Os(1)	0.5309(2)	0.5852(1)	0.4816(1)
Os(2)	0.4203(2)	0.4306(1)	0.5842(1)
Os(3)	0.2750(2)	0.5485(1)	0.4842(1)
Os(4)	0.4314(2)	0.4331(1)	0.3896(1)
Os(5)	0.6811(2)	0.4646(1)	0.3719(1)
C(11)	0.691(4)	0.617(3)	0.504(3)
C(12)	0.471(4)	0.676(3)	0.561(3)
C(13)	0.501(4)	0.658(3)	0.382(3)
C(21)	0.519(4)	0.344(3)	0.641(3)
C(22)	0.285(4)	0.353(3)	0.595(3)
C(23)	0.392(4)	0.503(3)	0.690(3)
C(31)	0.126(4)	0.489(3)	0.497(3)
C(32)	0.223(5)	0.633(4)	0.578(4)
C(33)	0.237(4)	0.630(3)	0.390(3)
C(41)	0.418(4)	0.486(3)	0.286(3)
C(42)	0.383(4)	0.314(3)	0.349(3)
C(51)	0.718(4)	0.414(3)	0.479(3)
O(11)	0.788(3)	0.644(2)	0.519(2)
O(12)	0.463(4)	0.744(3)	0.605(3)
O(13)	0.480(3)	0.712(2)	0.329(2)
O(21)	0.568(3)	0.282(2)	0.672(2)
O(22)	0.203(3)	0.309(2)	0.609(2)
O(23)	0.370(3)	0.546(3)	0.751(2)
O(31)	0.033(3)	0.458(3)	0.509(3)
O(32)	0.199(4)	0.683(3)	0.631(3)
O(33)	0.202(3)	0.675(2)	0.334(2)
O(41)	0.395(3)	0.526(3)	0.207(2)
O(42)	0.344(3)	0.249(2)	0.326(2)
O(51)	0.759(3)	0.377(2)	0.538(2)
C(1)	0.761(4)	0.585(3)	0.302(3)
C(2)	0.857(4)	0.531(3)	0.335(3)
C(3)	0.856(4)	0.432(3)	0.320(3)
C(4)	0.774(5)	0.394(4)	0.262(4)
C(5)	0.690(5)	0.454(4)	0.223(3)
C(6)	0.680(4)	0.545(3)	0.238(3)

Experimental

All the reactions were performed under an atmosphere of dry, oxygen-free nitrogen. Technical grade solvents were purified by standard procedures. The complexes [$Os_4H_4(CO)_{12}$],[11] [$Ru(C_6H_6)(MeCN)_3$][BF_4]$_2$[12] and [$Os(C_6H_6)(MeCN)_3$][BF_4]$_2$[13] were prepared by literature procedures. Mass spectra were recorded using a Kratos model MS 902, IR spectra on a Perkin Elmer 1710 FT-IR and ^1H NMR spectra on a Bruker WH 250 MHz spectrometer respectively.

Preparations.—[$Os_4H_4(CO)_{11}$]$^{2-}$ 1. The compound [$Os_4H_4(CO)_{12}$] (50 mg) was suspended in thf (10 cm^3) and a solution of K–Ph_2CO in thf was added dropwise with stirring until all [$Os_4H_4(CO)_{12}$] was dissolved and a clear orange solution resulted. After removal of solvent, the remaining orange-brown oil was dissolved in dichloromethane and used without further purification.

$[RuOs_4H_4(\eta^6\text{-}C_6H_6)(CO)_{11}]$ **2**. To a solution of the dianion **1** (50 mg) in dichloromethane (10 cm^3) was added $[Ru(C_6H_6)(MeCN)_3][BF_4]_2$ (25 mg) and the solution stirred for *ca.* 0.5 h. After removal of solvent, the solid residue was chromatographed by TLC using CH_2Cl_2–hexane (60:40) as eluent. The red cluster $[RuOs_4H_4(\eta^6\text{-}C_6H_6)(CO)_{11}]$ **2** was isolated as the major product (Found: C, 16.3; H, 0.8. Calc. C, 16.3; H, 0.8%), R_f 0.8, *ca.* 20% yield.

$[Os_5H_4(\eta^6\text{-}C_6H_6)(CO)_{11}]$ **3** *and* $[Os_5H_4(\eta^6\text{-}C_6H_6)(CO)_{12}]$ **4**. The methodology was analogous to that applied for **2**, using $[Os(C_6H_6)(MeCN)_3][BF_4]_2$ (25 mg). After removal of solvent, the solid residue was chromatographed by TLC using CH_2Cl_2–hexane (60:40) as eluent. The first red band was characterised as $[Os_5H_4(\eta^6\text{-}C_6H_6)(CO)_{11}]$ **3** (Found: C, 15.3; H, 0.7. Calc. C, 15.2; H, 0.7%), R_f 0.7, *ca.* 25% yield. The second green band was identified as $[Os_5H_4(\eta^6\text{-}C_6H_6)(CO)_{12}]$ **4** (Found: C, 15.8; H, 0.7. Calc. C, 15.8; H, 0.7%), R_f 0.5, *ca.* 25% yield.

X-Ray Analysis of Compounds **2**–**4**.—For structures **2** and **3** intensity data were collected on a Nicolet R3m/V diffractometer, on an Enraf-Nonius CAD4 diffractometer for **4**. For all the structures these data were corrected for Lorentz polarisation effects and for absorption by the ψ-scan method. The relevant data for the crystal structure analyses are summarised in Table 5. The structures were solved by a combination of direct methods and Fourier-difference techniques and refined on *F* by full-matrix least-squares analysis (using the SHELXTL PLUS program[14] for **2** and **3**, SDP program[15] for **4**). The hydrogen atoms of the co-ordinated benzene molecules were generated in their ideal positions (C–H 0.96 Å). Final atomic coordinates for the three structures are presented in Tables 6–8.

Additional material available from the Cambridge Crystallographic Data Centre comprises H-atom coordinates, thermal parameters and remaining bond lengths and angles.

Acknowledgements

C.-K. L. gratefully acknowledges the award of a Fellowship from the Croucher Foundation. W.-T. W. thanks the Hong Kong Research Grant Council (RGC) and the University of Hong Kong for financial support.

References

1 D. Braga, F. Grepioni, B. F. G. Johnson, J. Lewis, C. E. Housecroft and M. Martinelli, *Organometallics*, 1991, **10**, 1260.

2 (*a*) M. A. Gallop, B. F. G. Johnson, J. Lewis and P. R. Raithby, *J. Chem. Soc., Chem. Commun.*, 1987, 1809; (*b*) D. Braga, F. Grepioni, B. F. G. Johnson, E. Parisini, M. Martinelli, M. A. Gallop and J. Lewis, *J. Chem. Soc., Dalton Trans.*, 1992, 807.

3 A. T. Brooker, P. A. Jackson, B. F. G. Johnson, J. Lewis and P. R. Raithby, *J. Chem. Soc., Dalton Trans.*, 1991, 707.

4 H. Chen, B. F. G. Johnson, J. Lewis, D. Braga, F. Grepioni and E. Parisini, *J. Chem. Soc., Dalton Trans.*, 1991, 215.

5 D. Braga, F. Grepioni, P. Sabatino, P. J. Dyson, B. F. G. Johnson, J. Lewis, P. T. Bailey, P. R. Raithby and D. Stalke, *J. Chem. Soc., Dalton Trans.*, 1993, 985.

6 (*a*) M. P. Gomez-Sal, B. F. G. Johnson, J. Lewis, P. R. Raithby and A. H. Wright, *J. Chem. Soc., Chem. Commun.*, 1985, 1682; (*b*) D. Braga, F. Grepioni, B. F. G. Johnson, H. Chen and J. Lewis, *J. Chem. Soc., Dalton Trans.*, 1991, 2559.

7 R. Mason and W. R. Robinson, *Chem. Commun.*, 1968, 468.

8 S. J. Heyes, M. A. Gallop, B. F. G. Johnson, J. Lewis and C. M. Dobson, *Inorg. Chem.*, 1991, **30**, 3850; M. A. Gallop, M. P. Gomez-Sal, C. E. Housecroft, B. F. G. Johnson, J. Lewis, S. M. Owen, P. R. Raithby and A. H. Wright, *J. Am. Chem. Soc.*, 1992, **114**, 2503; M. A. Gallop, B. F. G. Johnson, J. Keeler, J. Lewis, S. J. Heyes and C. M. Dobson, *J. Am. Chem. Soc.*, 1992, **114**, 2510.

9 A. G. Orpen, *J. Chem. Soc., Dalton Trans.*, 1980, 2509.

10 G. R. John, B. F. G. Johnson, J. Lewis, W. J. H. Nelson and M. McPartlin, *J. Organomet. Chem.*, 1979, **171**, C14.

11 C. Zuccaro, *Inorg. Synth.*, 1989, **26**, 293.

12 M. A. Bennett and K. Smith, *J. Chem. Soc., Dalton Trans.*, 1974, 233.

13 Y. Hung, W.-J. Kung and H. Taube, *Inorg. Chem.*, 1981, **20**, 457.

14 SHELXTL PLUS™, Release 4.0, Siemens Analytical X-Ray Instruments, Madison, WI, 1990.

15 Enraf-Nonius Structure Determination Package, SDP, Enraf-Nonius, Delft, 1985.

Received 14*th October* 1992; *Paper* 2/05515E